Hydrothermal Prospection in the Red Sea Rift: Geochemical Messages from Basalts

Froukje M. van der Zwan, Colin W. Devey, and Nico Augustin

Abstract

Hydrothermal circulation at mid-ocean ridges and assimilation of hydrothermally altered crust or hydrothermal fluids by rising magma can be traced by measuring chlorine (Cl) excess in erupted lavas. The Red Sea Rift provides a unique opportunity to study assimilation of hydrothermally altered crust at an ultra-slow spreading ridge (maximum 1.6 cm yr^{-1} full spreading rate) by Cl, due to its saline seawater (40–42‰, cf. 35‰ in open ocean water), the presence of (hot) brine pools (up to 270‰ salinity and 68 °C) and the thick evaporite sequences that flank the young rift. Absolute chlorine concentrations (up to 1300 ppm) and Cl concentrations relative to minor or trace elements of similar mantle incompatibility (e.g., K, Nb) are much higher in Red Sea basalts than in basalts from average slow spreading ridges. Mantle Cl/Nb concentrations can be used to calculate the Cl-excess, above the magmatic Cl, that is present in the samples. Homogeneous within-sample Cl concentrations, high Cl/H_2O, the decoupling of Cl-excess from other trace elements and its independence of the presence of highly saline seafloor brines at the site of eruption indicate that Cl is not enriched at the seafloor. Instead we find basaltic Cl-excess to be spatially closely correlated with evidence of hydrothermal activity, suggesting that deeper assimilation of hydrothermal Cl is the dominant Cl-enrichment process. A proximity of samples to both evaporite outcrops and bathymetric signs of volcanism on the seafloor enhance Cl-excess in basalts. The basaltic Cl-excess can be used as a tracer together with new bathymetric maps as well as indications of hydrothermal venting (hot brine pools, metalliferous sediments) to predict where hydrothermal venting or now inactive hydrothermal vent fields can be expected. Sites of particular interest for future hydrothermal research are the Mabahiss Deep, the Thetis-Hadarba-Hatiba Deeps and Shagara-Aswad-Erba Deeps (especially their large axial domes), and Poseidon Deep. Older hydrothermal vent fields may be present at the Nereus and Suakin Deeps. These sites significantly increase the potential of hydrothermal vent field prospection in the Red Sea.

1 Introduction

1.1 Hydrothermal Circulation at (Ultra) Slow-Spreading Ridges

Hydrothermal circulation of seawater, driven by the magmatic heat of young oceanic lithosphere is an important process at all mid-ocean ridges (MORs). There, cold seawater that penetrates the crust provides an effective way to cool the newly formed oceanic crust. The fluids that get heated rise again to the seafloor, where hydrothermal activity can be expressed by diffuse (low temperature) or focussed (high temperature) venting in the form of (black or white) smoker fields. Interaction of the circulating seawater with the hot magma and rocks of the oceanic crust leads to a metal enrichment of the fluids. Upon cooling of these fluids at the surface this metal enrichment can build economically interesting seafloor massive sulphide (SMS) deposits (Rona et al. 1986; Hannington et al. 2011). In addition, the heat and specific chemistry of the venting fluids create habitats for chemosynthetic communities at the seafloor.

Hydrothermal activity occurs at all MORs, but the along-axis frequency of high temperature hydrothermal venting increases with spreading rate; calculations for (ultra) slow-spreading ridges, like the Red Sea Rift (<10–16 mm yr^{-1}; Chu and Gordon 1998) plot on the lower end and

F. M. van der Zwan (✉) · C. W. Devey · N. Augustin
GEOMAR Helmholtz Centre for Ocean Research Kiel, Wischhofstraße 1-3, 24148 Kiel, Germany
e-mail: fzwan@geomar.de

F. M. van der Zwan
Institute of Geosciences, Christian Albrechts University Kiel, Ludewig-Meyn-Straße 10, 24118 Kiel, Germany

N. M. A. Rasul and I. C. F. Stewart (eds.), *Geological Setting, Palaeoenvironment and Archaeology of the Red Sea*,
https://doi.org/10.1007/978-3-319-99408-6_10

indicate at least one active vent field every 100 km of ridge axis (e.g., Baker and German 2004; Hannington et al. 2011; Beaulieu et al. 2015). Moreover, ultraslow-spreading ridges such as the Gakkel Ridge and the Southwest Indian Ridge that were believed to be hydrothermally less active show—wherever investigated in more detail—more sites of active venting to be present than expected (e.g., Edmonds et al. 2003; German et al. 2016). Despite a lower along-axis frequency, the size of hydrothermal deposits at (ultra) slow-spreading ridges is generally larger compared to fast-spreading ridges (Fouquet 1997) and they have a higher Cu and Au potential, which makes them thus most attractive from an economic point of view (German et al. 2016). The largest known SMS deposits, like TAG and Semenov 4, have been discovered at the slow-spreading Mid-Atlantic Ridge (Petersen et al. 2000; Pertsev et al. 2012).

1.2 Current Inferred Sites of Hydrothermal Activity in the Red Sea

Hydrothermal venting in the Red Sea Rift (RSR) is inferred to occur in some of the Red Sea Deeps that contain highly saline (up to 270‰ NaCl) brine pools (e.g., Swallow and Crease 1965; Fig. 1). Although the brine pools are not of hydrothermal origin (Pierret et al. 2010; van der Zwan et al. 2015), the immobility of the dense pools gives them the capability to preserve and accumulate temperature and chemical attributes from hydrothermal fluids that are vented into a brine, in contrast to ambient seawater, where those attributes are quickly dispersed by the convecting seawater and can only be traced close to the source. The brine pools in the Red Sea vary in temperature from being similar to Red Sea bottom water (about 22 °C) up to 68 °C (in the Atlantis II Deep) and can have a characteristic chemical composition, for example up to 5 orders of magnitude higher trace element and gas concentrations compared to ambient Red Sea bottom water (e.g., Schmidt et al. 2015). High brine temperatures and specific chemistries are often associated with the occurrence of metalliferous sediments (Gurvich 2006, and references therein). In the Atlantis II Deep, the metalliferous sediments and their sulphur isotope compositions, together with the temperature and composition of the brine pool, suggest the strongest hydrothermal venting in the Red Sea into a brine (Bäcker and Richter 1973; Pierret et al. 2001; Laurila et al. 2014; Schmidt et al. 2015). With the large amount of metalliferous sediments, Atlantis II Deep is hosting the only known currently forming sedimentary exhalative ore (SEDEX) deposit in the world, underlining its hydrothermal origin. Besides Atlantis II Deep, the adjacent Discovery Deep and, further south, the Port Sudan Deep show metalliferous sediments and seafloor brine pools with elevated temperatures, indicating hydrothermal venting into

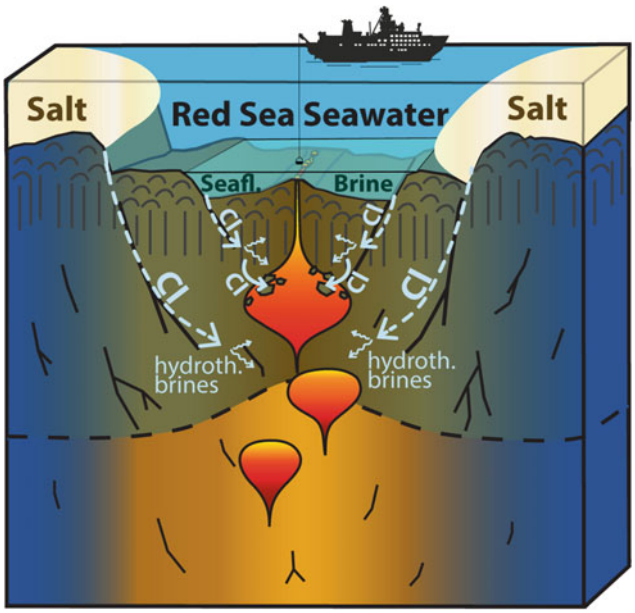

Fig. 1 Conceptual sketch showing the increase of Cl in the crust by hydrothermal alteration. The magmatic assimilation of hydrothermal fluids or hydrothermally altered crust causes a Cl gain in the magma leading to basalts with Cl-excess that can be dredged. High Cl in hydrothermal fluids is caused by phase separation (small arrows). Hydrothermal fluids interacting with evaporites or seafloor brines may be even more highly charged in Cl

the brine pools there as well (Pierret et al. 2001; Gurvich 2006; Schmidt et al. 2015). In addition, the Nereus Deep brine also shows elevated temperatures. Metalliferous sediments are not exclusively formed in Deeps with brines, but are always associated with hydrothermal activity (e.g. Thetis Deep; Pierret et al. 2010). Metalliferous sediments in some of these Deeps without brine pools or in Deeps with brine pools that have ambient temperatures (e.g., Shagara, Suakin Deeps) may suggest past occurrences of hydrothermal venting (Gurvich 2006; Pierret et al. 2010). Nevertheless, no active hydrothermal vents (black smokers) have been confirmed so far in the Red Sea by direct observation, due to the limited accessibility to the brine pools by modern camera sampling systems. Only some (extinct) black smokers and sulphide fragments have been reported from Kebrit Deep and from the 18°N RSR respectively (Monin et al. 1982; Blum and Puchelt 1991), but without any further indications of recent activity. From other areas on the RSR that do not host a brine pool, no information is known on hydrothermal venting due to a lack of detailed investigations.

This information implies that, even when counting the 3–4 inferred active vents in brines that are inaccessible for state-of-the-art, high-resolution visualisation equipment (underwater robots and autonomous vehicles), the number of active hydrothermal vent fields is significantly less than expected over the >1300 km length of the RSR. At this

spreading rate, we would expect a minimum of 13 active hydrothermal systems (based on the correlation between spreading rate and the statistical occurance of hydrothermal vents per 1000 km rift axis; Hannington et al. 2010, 2011; Beaulieu et al. 2015), which implies that there are more vent fields to be discovered in the Red Sea. The Red Sea may have an even further enhanced capacity for hydrothermal activity as the ocean crust has a significantly higher heat flow than other ultraslow-spreading ridges (Girdler and Evans 1977; Augustin et al. 2016). Each of these undiscovered fields is expected to contain considerable amounts of SMS due to the ultraslow-spreading rate of the RSR (cf. Fouquet 1997; Hannington et al. 2010, 2011). The unique high intrinsic seawater salinity (40–42‰ compared to 34.5‰ for average ocean water) of the Red Sea, the (hot) saline brine pools (Pierret et al. 2001), and thick evaporite sequences flanking the RSR (e.g., Whitmarsh et al. 1974; Mitchell et al. 2010; Augustin et al. 2014a; Fig. 1) likely result in highly saline hydrothermal fluids that may enhance fluid-rock chemistry exchange. The large tonnage of 90 Mt of metalliferous sediments (with up to 2.06% Zn, 0.46% Cu, 41 g/t Ag, and 3 g/t Au) in Atlantis II Deep shows the resource potential of a single RSR hydrothermal vent area (Guney et al. 1988; Laurila et al. 2014).

1.3 Hydrothermal Vent Field Prospection

Active high-temperature vent fields can be found by detecting their effluent in the overlying water column. This task can be performed by MAPR casts and Tow-Yos across the areas of interests (Klinkhammer et al. 1977; Baker and Massoth 1987; Edmonds et al. 2003; Devey et al. 2010) or by CTD-systems equipped with video-systems, water samplers and additional sensors (i.e., CH_4, CO_2, pH, Eh) that support visual ground-truthing of venting features and provide the opportunity for confirming, mapping and quantifying hydrothermal fluid input into the water column (Schmidt et al. 2013a; Linke et al. 2015). In addition, if a rough target area is known, vent fields can be detected using high-resolution sensors (Eh, turbidity, temperature, side-scan, magnetometer) from deep towed instrument platforms (TOBI) or autonomous underwater vehicles (AUV) that can provide measurements of water anomalies, magnetic anomalies and sidescan reflections over small areas. For detailed investigations those instruments can also directly image hydrothermal vent fields associated with hydrothermal plume signals (e.g., Blondel 2010; Szitkar et al. 2015). However, the search for hydrothermal fields using these methods is a difficult and time-consuming process, particularly due to the scarcity of detailed maps of the ocean floor. The discovery of extinct hydrothermal fields that are economically interesting and give information on hydrothermal activity over a longer time span, is at best extremely challenging.

As all hydrothermal venting is the seafloor expression of deep hydrothermal fluid circulation and alteration of the crust, an alternative prospection method for finding active and ancient, now inactive hydrothermal occurrences is to search for geochemical traces of deeper hydrothermal alteration of the crust. Evidence from fast-spreading ridges shows that hydrothermal activity and high-temperature alteration of the oceanic crust can indirectly be traced by the chemistry of submarine erupted mid-ocean ridge basalts (MORB) for which chlorine (Cl) is specifically indicative. This is because the Cl contents of seawater and magma are vastly different (1.9 wt% and generally <500 ppm respectively; Michael and Schilling 1989; Michael and Cornell 1998). Seawater infiltration and interaction with the oceanic crust will hence increase the Cl content of the crust by hydrothermal alteration (Barnes and Cisneros 2012; Fig. 1). Assimilation of this hydrothermally altered crust or of hydrothermal fluids (inclusions) by rising magma can subsequently increase the Cl content of this magma that later can be recovered as basalt from the seafloor (Fig. 1; e.g., Michael and Schilling 1989; Coogan et al. 2002; Gillis et al. 2003). Therefore, Cl in erupted lavas is a sensitive tracer for hydrothermal activity. Chlorine addition due to interaction of basalts with hydrothermal fluids was previously identified at fast-spreading mid-ocean ridges (e.g., Michael and Schilling 1989; Gillis et al. 2003; le Roux et al. 2006; France et al. 2009, 2010; Kendrick et al. 2013), in ophiolites (Coogan et al. 2002; Coogan 2003), at back-arc basins (Kent et al. 2002; Sun et al. 2007), as well as in ocean island basalts (Kent et al. 1999a, b; Kendrick et al. 2017).

The Cl concentrations in basalts from (ultra) slow-spreading ridges like the RSR are relatively low (Cl ~50–200 ppm), compared to fast-spreading ridges (Cl <1300 ppm; e.g., Michael and Cornell 1998). Nevertheless, using a high-precision method to measure Cl in basalts (van der Zwan et al. 2012) reveals that at slow-spreading ridges variations in Cl due to the assimilation of hydrothermal Cl can also be observed (van der Zwan 2014; van der Zwan et al. 2015, 2017). Furthermore, the highly saline environment of the Red Sea has the potential to create circulating hydrothermal fluids with high Cl contents (Fig. 1); therefore, the Cl contamination in basalts by hydrothermal circulation can be much higher than on average for (ultra)slow-spreading ridges. By obtaining Cl data (ranging from 50 to 1400 ppm) from Red Sea basalts by our high precision Cl measurement routine (±1–2 ppm SD) with low detection limits (~10 ppm; van der Zwan et al. 2012), we can use Cl enrichment in basalt as an excellent magmatic marker of present and past hydrothermal circulation that can be used to trace hydrothermalism in the RSR.

To encircle the potential locations of hydrothermal venting further, the geomorphological features along mid-ocean ridges can be analysed, in order to predict potential locations of hydrothermal venting (Yoshikawa et al. 2012). At (ultra)slow-spreading ridges, hydrothermal vent fields have often been found at two specific types of rift morphologies. All closely investigated oceanic core complexes revealed ultramafic hosted vent fields (www.interridge.org; Früh-Green et al. 2003; Petersen et al. 2009; Pertsev et al. 2012; Escartín et al. 2017), but core complexes have not been identified in the RSR so far (Augustin et al. 2016). Many basalt-hosted hydrothermal systems at (ultra) slow-spreading ridges are related to large axial volcanoes, highs and volcanic ridges (Lein et al. 2010; Fontaine et al. 2014; Anderson et al. 2016). For example, along the Mid-Atlantic Ridge at 13–33 °S all large axial volcanoes show active hydrothermal venting (Devey et al. 2013). These axial volcanoes have a relatively smooth surface, indicating recent volcanic activity, and are remarkably similar in their morphological appearance to the axial domes found in the RSR (Augustin et al. 2016). Here the use of the latest high-resolution bathymetry data of the RSR (Augustin et al. 2014a, b, 2016) together with targets derived from hydrothermal Cl-excess in basalt and additional indicators for the occurrence of hydrothermal activity in the RSR (hot brine pools, metalliferous sediments) enable us to define the most promising areas for currently active and older, inactive hydrothermal vent fields and to evaluate hydrothermal activity in the Red Sea.

2 Chlorine Excess in Red Sea Basalts

The samples are derived from 25.5°N to 16.5°N on the RSR (van der Zwan et al. 2015) and are dredged basalts that come in the form of pillow lavas, lobate and sheet lavas or rock fragments with glassy surfaces (Fig. 2). The freshest (and therefore likely youngest) samples (with no visible alteration) were collected from Erba Deep (Fig. 2a), while some samples from Atlantis II (Fig. 2b) and all samples from

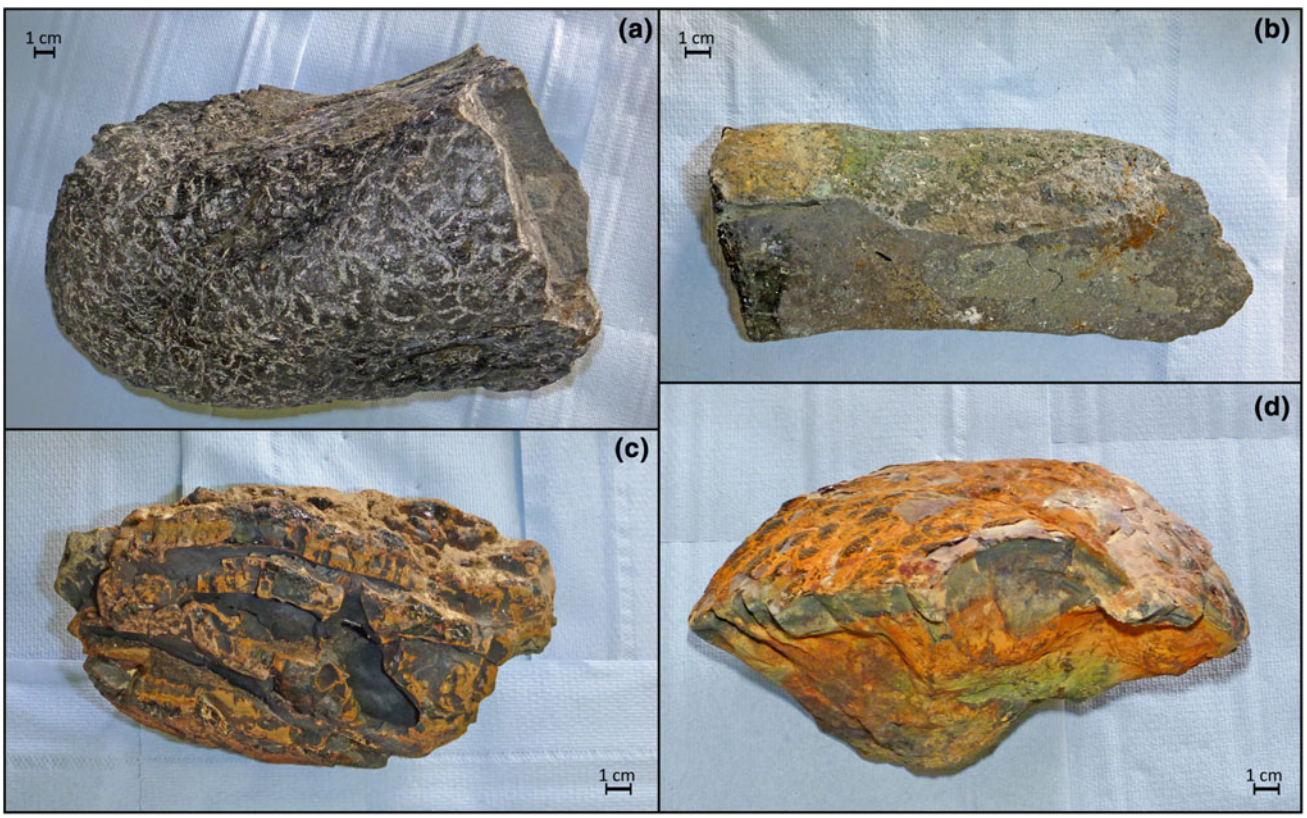

Fig. 2 Examples of basalt samples from the Red Sea. **a** Freshest recovered pillow basalt from Erba Deep (64PE350-43DR). The salt encrustations (whitish network on the rock) show that the basalt was recovered from a seafloor brine. **b** Blocky basalt from within Atlantis II Deep (64PE350-33DR) shows most alteration, but nevertheless has fresh glass on the top (left in the picture). **c** Basalt from Mabahiss Deep (64PE351-14DR) shows sheet flows with fresh glass under a thin palagonite layer. **d** Well-formed pillow basalt from Hadarba Deep (64PE350-23DR) with a fine crystalline interior but fresh glasses on top under a thin palagonite layer

Shaban Deep show the strongest alteration, although they still contain fresh glass. The samples from Erba and Northern Atlantis II Deeps were recovered out of the seafloor brine pools (Schmidt 2013b). Fresh glasses from the rocks have been selected and analysed for Cl, major and trace elements by electron microprobe and laser-induced-coupled-plasma-spectrometer (for details see van der Zwan et al. 2015). The analytical precision (2 standard deviations) for Cl is generally <3 ppm, for major elements <2.5%, but up to 5% for Na and MgO and ~30% for Mn and P and typically <2–5% (one standard deviation) for trace elements. The reproducibility is 1–2 ppm for internal standards (van der Zwan et al. 2012).

Red Sea glasses are both on grain and sample scale very homogeneous in their Cl, major and trace element concentrations, without any gradients. The samples have Cl values that range from 58.7 to 1399 ppm (van der Zwan et al. 2015) that are elevated compared to the majority of other slow-spreading ridges (<200 ppm; Michael and Cornell 1998). To determine the amount of Cl enrichment by hydrothermal processes, without disturbing this signal by variations in magmatic Cl, it is important to estimate the amount of magmatic Cl in each of the samples. As magmatic Cl concentrations vary with melting or crystallisation processes, we can use elements that behave similarly during these processes, that is, with a similar mineral-melt distribution coefficient, such as K or Nb to estimate the magmatic Cl concentrations (Sun et al. 2007). As Nb is the closest to Cl in incompatibility and less mobile than K, we prefer to use the Cl/Nb ratio from the mantle (that will not be changed during magmatic processes as the elements behave similarly) to calculate magmatic Cl from Nb. The global Cl/Nb mantle ratio is <30 (e.g., McDonough and Sun 1995; Saal et al. 2002; le Roux et al. 2006), but varies with region. For the Red Sea, the Cl/Nb ratio can be refined based on the lowest measured Cl/Nb values of the samples, since neither magmatic processes, nor interaction with seawater can explain a lower Cl/Nb than the mantle Cl/Nb ratio (Fig. 3a). This mantle ratio seems to be homogeneous in the Red Sea, as Cl/Nb is not correlated with any trace elements or trace element ratios that indicate source processes (van der Zwan et al. 2015). The lowest Cl/Nb samples of the Red Sea fall over a range of compositions with Nb from 1 to 35 ppm on a line of 18.3 ± 2.5 that can be taken as the maximum Cl/Nb mantle value (Fig. 3a), and which falls within the range of Cl/Nb mantle values in the literature (see discussion in van der Zwan et al. 2017). The samples that coincide with this line do not show Cl-excess; for all other samples, the magmatic Cl can be calculated and from that the amount of Cl-excess, by extracting the magmatic Cl from the measured Cl using the formula: $Cl_{excess} = Cl_{measured} - (Cl/Nb_{mantleRedSea} \times Nb_{measured})$. The result is shown in Fig. 3b and shows that in contrast to Cl/Nb ratios, the Cl-excess is independent from the Nb content of the samples (and hence their magmatic Cl content), thereby excluding any magmatic effects. The Cl-excess in the Red Sea basalts is visible in 84% of the samples and ranges from 15 ppm up to 1340 ppm (Fig. 3b). Cl-excess is present in samples from the entire RSR apart from the RSR at 17°N, but is more evident at the Hadarba, Hatiba, Atlantis II, Discovery, Aswad and Port Sudan Deeps (Fig. 4).

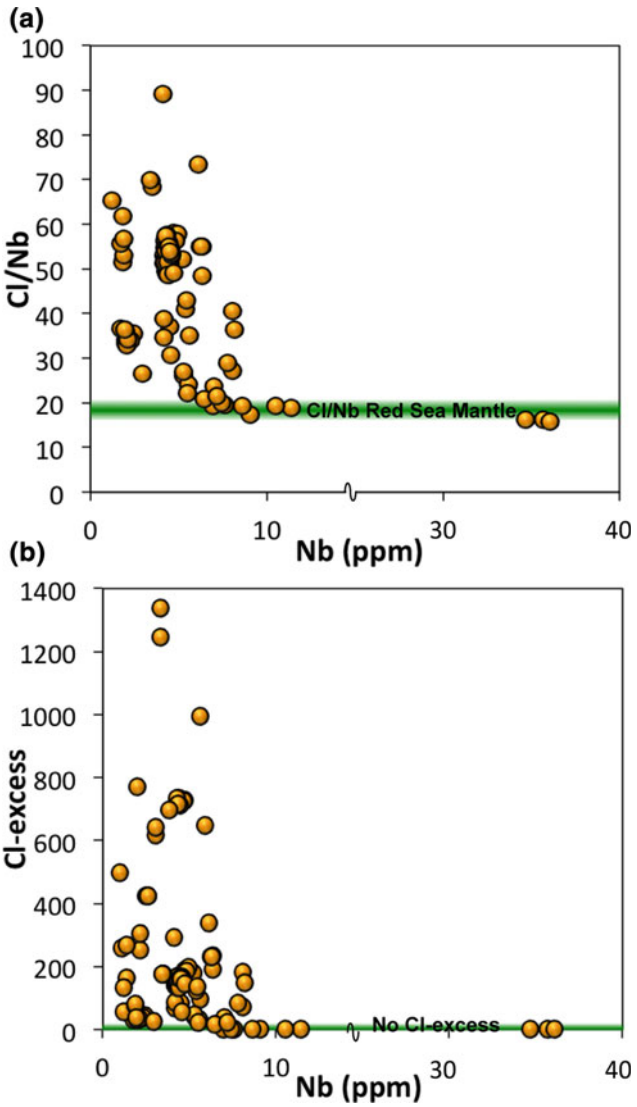

Fig. 3 Chlorine chemistry of the Red Sea basalts. **a** Cl/Nb versus Nb of the samples compared to the Cl/Nb of the Red Sea mantle shows strongly elevated Cl values for most samples. **b** Calculated Cl-excess against Nb reveals that most samples have Cl-excess which is independent of the trace element chemistry (Nb-content) of the samples

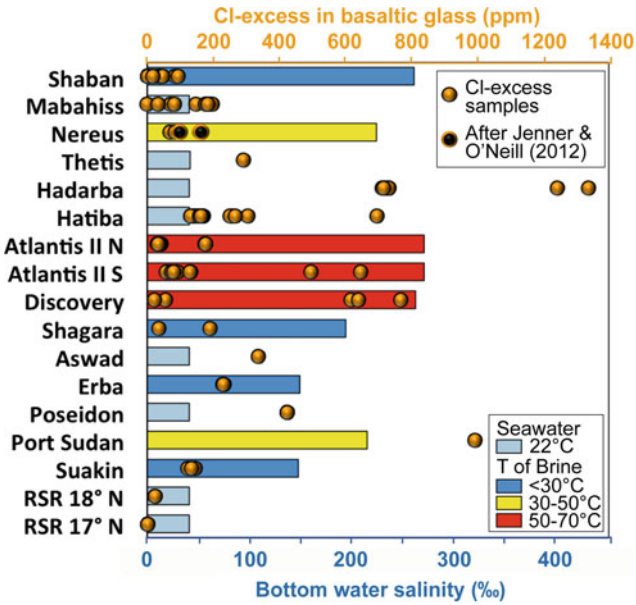

Fig. 4 Cl-excess of basalts (dots; this study used data from van der Zwan et al. 2015 and additionally Cl-excess after data of Jenner and O'Neill 2012 is shown) grouped by geographic location along the RSR, compared to local bottom water salinity (bars) and temperatures (indicated by the colour of the bars). Brines with high temperatures consistently contain some basalts with Cl-excess (100–800 ppm), indicating that basaltic Cl-excess shows hydrothermal activity in the crust

3 Discussion

3.1 Chlorine Excess and its Relation to Hydrothermal Activity and Venting

By using Cl-excess above the magmatic Cl contents, we are able to exclude variations in mantle Cl contents and the effects of crustal magmatic processes on the Cl contents. Therefore, any Cl-excess should occur due to the interaction of magma with seawater (cf. Jambon et al. 1995). Interaction with seawater would be possible at the seafloor, either post-eruptive, by direct low temperature alteration (e.g., Hart et al. 1974), or syn-eruptive, by incorporation of vaporized seawater in sheet lavas during emplacement (Perfit et al. 2003; Soule et al. 2006). However, for the Red Sea basalts Cl addition at the seafloor is excluded based on: (I) The fresh appearance of the glass chips and lack of pervasive alteration (minerals); (II) Some of the optically most altered samples (Shaban, Atlantis II Deeps) show the lowest Cl-excess, while the freshest samples from Erba Deep show significant Cl-excess (Figs. 2 and 4); (III) Homogeneous Cl-excess in the samples is not consistent with alteration, where gradients would be expected; (IV) The lack of any correlation of Cl to chemical indicators of surficial alteration (e.g., U, Ba, Pb, Rb; Alt et al. 1986; Alt and Teagle 2003; Schramm et al. 2005; Augustin et al. 2008); (V) Samples that display Cl-excess have lower H_2O contents than expected for pure seawater alteration (cf. Ito et al. 1983; Staudigel et al. 1996; Bach et al. 2003; le Roux et al. 2006). To generate the observed Cl-excess in basalts without significantly elevating the H_2O contents of the samples requires a salty contaminant with Cl/H_2O ratios of >0.25, which is higher than seawater ($Cl/H_2O_{seawater}$ ~0.02) or the seafloor brines ($Cl/H_2O_{seafloor\ brine}$ <0.22) (for details see van der Zwan et al. 2015). In addition, we see no systematics in Cl-excess for samples that are recovered from brine pools or from ambient seawater (Fig. 4).

Since Cl addition due to interaction with seawater at the seafloor can be excluded, Cl must have been added deeper in the crust. This is consistent with homogenous Cl contents within each of the samples that suggest mixing and homogenisation of magma after Cl incorporation as shown by van der Zwan et al. (2015). The Cl contaminant, which must have a relatively high Cl/H_2O ratio, cannot be simply heated seawater. Neither does bulk hydrothermally altered crust have a high enough Cl/H_2O ratio to produce the observed Cl-excess when assimilated (<0.036; Ito et al. 1983; Bach et al. 2003; Barnes and Cisneros 2012; van der Zwan et al. 2015). Fluids with high Cl/H_2O ratios are found in the crust in the form of hydrothermal brines with up to 50% salinity (not to be confused with the seafloor brines) that are formed by phase separation of heated seawater (Bischoff and Rosenbauer 1987; Fournier 1987; Kelley and Delaney 1987; Berndt and Seyfried 1990; Von Damm et al. 2003; Fig. 1). Chlorine from these hydrothermal brines can be added to a magma in diverse ways. They can be directly incorporated as a liquid into a magma (Kendrick et al. 2013), or by assimilation of hydrothermally altered crust, if brine fluids are present in the porosity of the rocks (Coogan et al. 2003; Gillis et al. 2003). Also in high-Cl hydrothermally formed minerals such as amphibole (Barnes and Cisneros 2012), brines can be present in the form of brine inclusions or in the crystal structure, which provides an alternative mechanism to add Cl to a melt if this altered crust is assimilated (Michael and Schilling 1989; Kent et al. 1999a). Assimilation of only partial melts of hydrothermally altered crust, which are particularly formed by these secondary Cl and/or brine-rich minerals that have the lowest solidus temperatures, will also result in high Cl/H_2O liquids as the melt takes up more Cl than H_2O (Kent et al. 1999a; France et al. 2010; Wanless et al. 2010). In all cases, even though the exact mechanism to incorporate Cl that was introduced by hydrothermal fluids in the sub-surface to a magma is disputed, the resulting erupted basalts with Cl-excess indicate hydrothermal activity.

This is confirmed by a comparison of Cl-excess in basalts to sites with other, independent evidence for hydrothermal activity. The Red Sea data show that Cl-excess related to

hydrothermal activity is widespread all along the RSR, demonstrating that hydrothermal circulation is occurring everywhere along the ridge to a certain degree. However, we see a clear variation in Cl-excess between samples from different locations. The high variation in Cl-excess between samples, also within a Deep, reflects the high compositional variety with heterogeneous amounts of hydrothermal alteration of slow-spreading oceanic crust and the relatively small scale of processes acting there (e.g., Dick et al. 2000). As hydrothermal circulation is not pervasive throughout the crust and magmas may assimilate different sections of this crust, the lack of Cl-excess does not preclude hydrothermal circulation, but samples with Cl-excess always point to interaction with hydrothermal brines. The regions in the Red Sea with evidence for focussed former or present-day seafloor extrusion of hydrothermal fluids in the form of metalliferous seafloor precipitates (e.g., Thetis, Shagara and Suakin Deeps) and/or hot brine pools (Nereus, Atlantis II, Discovery and Port Sudan Deeps; red and yellow bars in Fig. 4) always yielded basalts with the highest Cl-excess of >100 ppm (Cl/Nb >50; van der Zwan et al. 2015). Within the Atlantis II Deep samples with the strongest Cl-excesses are found close to the SW basin and on the western flank of Discovery Deep (van der Zwan et al. 2015), areas where most probably current hydrothermal venting into the brine is occurring, based ontrace element studies (Brewer and Spencer 1969; Bäcker and Schoell 1972; Schoell and Hartmann 1973; Monin et al. 1981). This suggests that on the scale of a single Deep, high Cl-excess in basalt can also indicate the location of hydrothermal venting. In conclusion, Cl-excess in basalts can be used as a firm indicator of the strongest (past and present) hydrothermal circulation and the amount of Cl-excess can be applied to indicate potential areas affected by hydrothermal venting (cf. van der Zwan et al. 2015, 2017).

3.2 Red Sea Morphology and Cl-Excess in Basalts

Chlorine excess due to hydrothermal activity in Red Sea basalts is strongly linked to the morphological features of the Red Sea Rift, particularly to volcanic activity and the proximity to evaporites on the rift flanks. Samples with the highest Cl-excess (>250 ppm; Cl/Nb >100; van der Zwan et al. 2015) are always found within 5 km distance of evaporites, indicating that close to evaporites the inflowing water becomes highly charged with Cl as a result of evaporite dissolution and 5 km may be indicative of the scale of the recharge zone. Beyond 5 km, Cl-excess is still obvious but less strong, representing hydrothermal alteration of the crust by circulation of ambient Red Sea bottom water. When evaluating the areas for the best hydrothermal prospection, it needs to be kept in mind that some of the extreme values may be a result of evaporite presence and therefore not directly indicative of the strongest hydrothermal activity or the location of vent fields. More indicative for hydrothermal vent field prospection is the relation between Cl-excess and volcanism.

It was shown that magmatic intensity based on the percentage area of volcanic edifices and ridges, discernible in seafloor morphology, has a positive relation with Cl-excess in Red Sea basalts (van der Zwan et al. 2015). In addition, we note that in the Thetis-Hadarba-Hatiba area, which was determined by Augustin et al. (2016) to be the most volcanically active area in the central Red Sea, some of the highest Cl-excess in basalts is found (Fig. 4). The fact that the southern RSR, which is volcanically even more active, does not show the same Cl-excess has likely to do with the absence of evaporites close by (van der Zwan et al. 2015). In the central RSR faults are not related to Cl-excess and are probably ubiquitously present so that the pathways for hydrothermal activity are always available (van der Zwan et al. 2015). As shown by the relation between volcanism and Cl-excess, here the presence or absence of a heat source (volcanic activity) is essential for hydrothermalism to take place. Strong and robust magmatism that has been active since several Ma can be found in the Red Sea in the form of large axial dome volcanoes (Mabahiss Mons, Thetis Dome, Hatiba Mons, Aswad Dome) and associated spreading-perpendicular volcanic ridges (Metz et al. 2013; Augustin et al. 2014b, 2016). These domes are very similar to large dome volcanoes at other (ultra)slow-spreading ridges that host active hydrothermal vent systems, such as at the southern (Devey et al. 2013) and northern Mid-Atlantic Ridge (Marcon et al. 2013; Escartín et al. 2014). Indeed, the domes in the Red Sea show recent activity in the form of lava flows that are visible in multibeam backscatter data (Augustin et al. 2016) and all hosted basalts display Cl-excess (Fig. 4). This demonstrates that geomorphological evidence for high volcanic activity can be used together with the Cl-excess to point to the most promising areas where hydrothermal venting is presently taking place.

3.3 Hydrothermal Vent Field Potential of the Red Sea Rift

With the new advances in the geomorphology of the RSR and the geochemistry of its basalts, we are able to make a contemporary evaluation of the present (and past) areas influenced by hydrothermal activity along the RSR (Fig. 5). For this we used previously known indications for hydrothermal activity such as the temperatures of the brines and occurrences of metalliferous sediments in the deeps, together with new information of basaltic Cl-excess and the

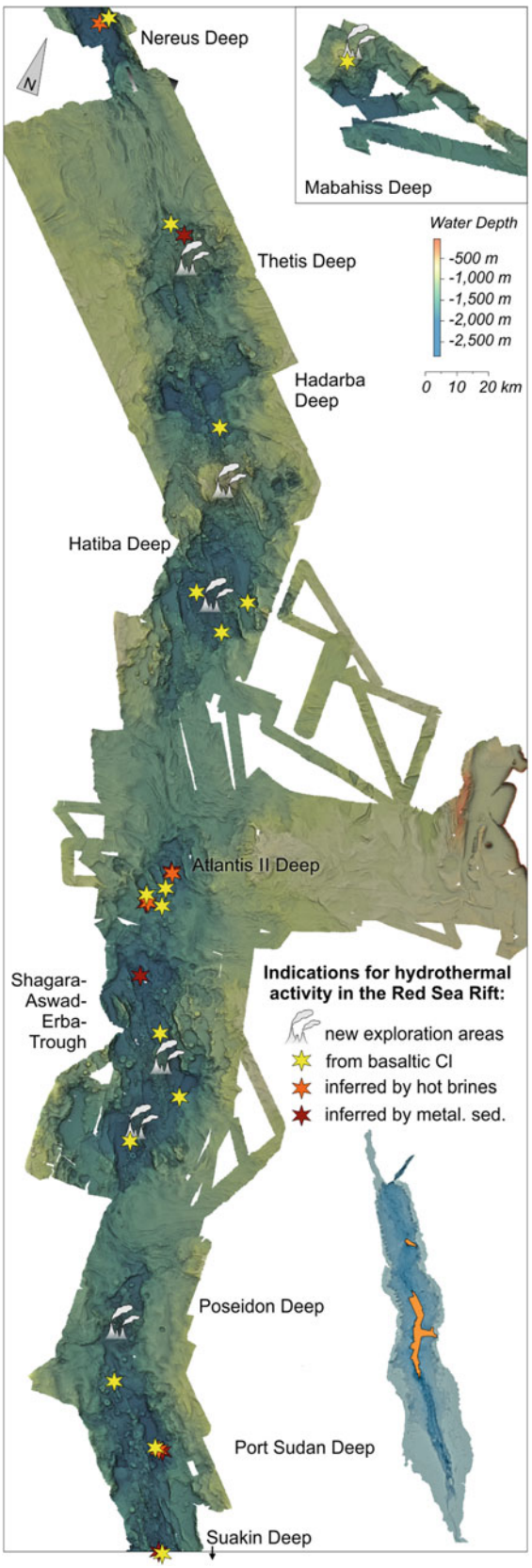

Fig. 5 Bathymetric map of the central RSR with inferred sites of hydrothermal activity based on basaltic Cl-excess (yellow stars), brine temperatures (orange stars) and metalliferous sediments (red stars). New exploration areas based on Cl-excess and rift morphology are also indicated (smokers)

latest bathymetric models of the RSR. While the metalliferous sediments and Cl-excess give information on the possible occurrence of massive sulphide deposits formed by hydrothermal activity at any possible time, the temperatures of the brines and indications from morphology for recent or past volcanism (providing a heat source to drive hydrothermalism) give insights as to whether hydrothermal venting at these locations may be current or extinct.

In the previous paragraphs, we have shown that all sites that have high temperature seafloor brine pools (Atlantis II, Discovery and Port Sudan, Nereus Deeps; red and yellow bars in Fig. 4) and hence must have hydrothermal venting into the brine, also have high basaltic Cl-excess. However, we see differences between the locations, with Nereus Deep showing clearly lower Cl-excess in its rock samples and having the lowest elevated brine temperature (30°; Schmidt et al. 2015). Bathymetry from Nereus Deep shows little evidence of active volcanism, and a greater depth of the Deep (Fig. 5). Also, basalt samples collected from there were embedded in carbonates and thus are older. This implies that hydrothermal venting is presently limited in Nereus Deep, due to the lack of recent volcanism. In the other high-temperature brines, venting seems very active, also shown by the abundant metalliferous sediments there and increasing brine temperatures of the Atlantis II Deep brines during the last decades (Schmidt et al. 2015).

At Shagara, Erba and Suakin Deeps hydrothermal activity is indicated by Cl-excess and in some cases metalliferous sediments, but the seafloor brines are colder (within 5 °C of ambient temperatures; Fig. 4). Thus, although hydrothermal activity is indicated, this is either not presently active, or venting is not taking place within the brine pool. The first is most likely the case for Suakin Deep, which is at present the deepest area of the whole RSR and characterised by extensive tectonic and little volcanic activity (Fig. 5); only 5% of the area shows high multibeam backscatter indicating recent volcanism (Augustin et al. 2014a, b). Also, samples recovered from here indicate older ages as they were covered by thick manganese encrustations, indicating former volcanism and hydrothermal venting. Samples from Shagara and Erba Deeps, in contrast, are fresh glasses with Cl-excess coupled with higher volcanic activity and recent lava flows seen in backscatter data (Augustin et al. 2014b, 2016; Fig. 5). Here hydrothermal venting is most likely presently occurring outside of the brine pools (and therefore any heat released through focussed venting is released to ambient seawater and not trapped in the brine pools), perhaps not surprisingly in view of their relatively small volume (≤ 11 km^2) compared to their large basins (>800 km^2). In these Deeps, recent hydrothermal venting seems likely and they represent good targets for hydrothermal prospection for non-brine-covered vent fields. Shaban Deep, which also hosts a cool brine pool, does not show any evidence of hydrothermal activity, other than low Cl-excess, which probably merely represents diffuse background hydrothermal circulation and does not represent the presence of focussed hydrothermal venting, leading to black smokers.

Chlorine-excess as an indicator of hydrothermal activity is most valuable for the areas in the RSR that do not host brine pools, as little other evidence is present there due to the lack of brines to store signals of hydrothermal venting and the few investigations of these areas. The strongest indications for hydrothermal activity from Cl-excess come from basalts of the Thetis-Hadarba-Hatiba Deeps area, which is hence a primary target for hydrothermal exploration (Figs. 4 and 5). This area also displays a comparably shallow rift axis and discernible volcanic edifices cover 44% of the seafloor (average of the RSR is ~33%), with 20% displaying fresh lava flows (Augustin et al. 2016). This implies that sufficient heat must have been available to drive hydrothermal circulation and that hydrothermal activity is most likely recent. In more detail, the highest Cl-excess is found in Hadarba deep close to the largest dome volcano, Hatiba Mons (Fig. 5), confirming the relation between hydrothermal activity and dome volcanoes. Moreover, the other large volcanoes on the RSR (Thetis Dome, Aswad Dome and Mabahiss Mons) are interpreted to host hydrothermal venting, due to their strong association with Cl-excess and additionally the occurrence of metalliferous sediments in the Thetis Deep. As volcanism seems to be active at all domes based on recent lava flows and fresh samples (Metz et al. 2013; Augustin et al. 2016), hydrothermal venting is also likely to be presently active there. Another volcanically active area that hosts basalts with strong Cl-excess is 20 km north of Port Sudan Deep (Poseidon Deep), indicating possible current hydrothermal venting (Fig. 5).

In the southern Red Sea, Cl-excess is lower, due to the lack of evaporites and also high trace element concentrations (and thus high magmatic Cl), which makes it more difficult to detect Cl-excess. Nevertheless, Cl-excess is visible in some basalts at 18°N, consistent with fragments of sulphide chimneys, indicating hydrothermal vents there (Monin et al. 1982). Although bathymetric data show considerable volcanism, hydrothermal venting may have been present only for a limited time, due to the higher magmatic activity of the crust that may make it less permeable, comparable to variations observed at 5–11 °S MAR (Devey et al. 2010). With the current data, we therefore cannot determine whether or not this hydrothermal venting is occurring now.

4 Conclusions

Chlorine-excess in basalts shows that the RSR is hydrothermally active all along the axis. However, the temporal and spatial intensity of this activity is varying and

focussed hydrothermal venting is only indicated by higher basaltic Cl-excess. The target areas derived from Cl-excess in basalt, together with the good bathymetric data of the Red Sea Rift and additional indicators for the occurrence of hydrothermal activity in the RSR (hot brine pools, metalliferous sediments), enable us to define the most promising locations for hydrothermal vent fields and associated seafloor massive sulphide deposits and vent communities. The data shows that hydrothermal venting is probably currently occurring at Mabahiss Mons, in the Thetis-Hadarba-Hatiba Trough and the Shagara-Aswad-Erba Trough (particularly at the large axial volcanic Thetis Dome, Hatiba Mons and Aswad Dome) and in Poseidon Deep, in addition to previously known locations in the Atlantis II, Discovery and Port Sudan Deeps. Older hydrothermal vent fields may be present at Nereus and Suakin Deeps, while at the RSR at 18°N it is unclear if hydrothermal venting is still taking place. Our new evidence for hydrothermal activity significantly increases the potential of hydrothermal vent field prospection in the Red Sea and these new sites will be of particular interest for future hydrothermal research in the Red Sea.

Acknowledgements We are grateful for the help of the captains, crews and scientific shipboard parties of RV Poseidon and RV Pelagia expeditions P408 and PE350/351. We gratefully thank Jan Fietzke for the help with the Cl measurements and Mario Thöner, Matthias Frische, Dagmar Rau (all at GEOMAR) and Renat Almeev (University of Hannover) for technical support with the EMP, LA-ICP-MS and FTIR measurements, respectively. Antoine Bézos (University of Nantes) and Anna Krätschell are thanked for providing additional (sub)samples of the Red Sea. Reviews by three anonymous reviewers are greatly appreciated. We thank the Saudi Geological Survey for accommodating the workshop in preparation of this volume. We would like to acknowledge generous financial support from the Jeddah Transect Project, between King Abdulaziz University and Helmholtz-Centre for Ocean Research GEOMAR, that was funded by King Abdulaziz University (KAU), Jeddah, Saudi Arabia, under grant no. T-065/430.

References

Alt JC, Teagle DA (2003) Hydrothermal alteration of upper oceanic crust formed at a fast-spreading ridge: mineral, chemical, and isotopic evidence from ODP Site 801. Chem Geol 201:191–211

Alt JC, Honnorez J, Laverne C, Emmermann R (1986) Hydrothermal alteration of a 1 km section through the upper oceanic crust, Deep Sea Drilling Project Hole 504B: mineralogy, chemistry and evolution of seawater-basalt interactions. J Geophys Res Solid Earth 91:10309–10335

Anderson MO, Hannington MD, Haase K, Schwarz-Schampera U, Augustin N, McConachy TF, Allen K (2016) Tectonic focusing of voluminous basaltic eruptions in magma-deficient backarc rifts. Earth Planet Sci Lett 440:43–55

Augustin N, Lackschewitz K, Kuhn T, Devey CW (2008) Mineralogical and chemical mass changes in mafic and ultramafic rocks from the Logatchev hydrothermal field (MAR 15 N). Mar Geol 256:18–29

Augustin N, Devey CW, van der Zwan FM, Feldens P, Bantan RA, Kwasnitschka T (2014a) The rifting to spreading transition in the Red Sea. Earth Planet Sci Lett 395:217–230

Augustin N, Schmidt M, Devey CW, Al-Aidaroos A, Kürten B, Eisenhauer A, Brückmann W, Dengler M, van der Zwan FM, Feldens P (2014b) The Jeddah Transect Project: extensive mapping of the Red Sea Rift. InterRidge News 22:68–73

Augustin N, van der Zwan FM, Devey CW, Ligi M, Kwasnitschka T, Feldens P, Bantan RA, Basaham AS (2016) Geomorphology of the central Red Sea Rift: determining spreading processes. Geomorph 274:162–179

Bach W, Peucker-Ehrenbrink B, Hart SR, Blusztajn JS (2003) Geochemistry of hydrothermally altered oceanic crust: DSDP/ODP Hole 504B—implications for seawater-crust exchange budgets and Sr-and Pb-isotopic evolution of the mantle. Geochem Geophys Geosyst 4(3). https://doi.org/10.1029/2002gc000419

Bäcker H, Richter H (1973) Die rezente hydrothermal-sedimentäre Lagerstätte Atlantis-II-Tief im Roten Meer. Geol Rundsch 62:697–737

Bäcker H, Schoell M (1972) New deeps with brines and metalliferous sediments in the Red Sea. Nat Phys Sci 240:153–158

Baker ET, German CR (2004) On the global distribution of hydrothermal vent fields. In: German CR, Lin J, Parson LM (eds) Mid-ocean ridges: hydrothermal interactions between the lithosphere and oceans, vol 148. American Geophysical Union, Geophys Monograph, pp 245–266

Baker ET, Massoth GJ (1987) Characteristics of hydrothermal plumes from two vent fields on the Juan de Fuca Ridge, northeast Pacific Ocean. Earth Planet Sci Lett 85(1):59–73

Barnes JD, Cisneros M (2012) Mineralogical control on the chlorine isotope composition of altered oceanic crust. Chem Geol 326–327:51–60

Beaulieu SE, Baker ET, German CR (2015) Where are the undiscovered hydrothermal vents on oceanic spreading ridges? Deep Sea Res Part II 121:202–212

Berndt ME, Seyfried WE (1990) Boron, bromine, and other trace elements as clues to the fate of chlorine in mid-ocean ridge vent fluids. Geochim Cosmochim Acta 54:2235–2245

Bischoff JL, Rosenbauer RJ (1987) Phase separation in seafloor geothermal systems; an experimental study of the effects on metal transport. Am J Sci 287:953–978

Blondel P (2010) The handbook of sidescan sonar. Springer Science & Business Media

Blum N, Puchelt H (1991) Sedimentary-hosted polymetallic massive sulfide deposits of the Kebrit and Shaban Deeps, Red Sea. Mineral Depos 26:217–227

Brewer PG, Spencer DW (1969) A note on the chemical composition of the Red Sea brines. In: Degens ET, Ross DA (eds) Hot brines and recent heavy metal deposits in the Red Sea. Springer, Berlin, pp 174–179

Chu D, Gordon RG (1998) Current plate motions across the Red Sea. Geophys J Int 135:313–328

Coogan LA (2003) Contaminating the lower crust in the Oman ophiolite. Geology 31:1065–1068

Coogan LA, Mitchell NC, O'Hara MJ (2002) Roof assimilation at fast spreading ridges: an investigation combining geophysical, geochemical, and field evidence. J Geophys Res 108:2002

Coogan LA, Mitchell NC, O'Hara MJ (2003) Roof assimilation at fast spreading ridges: an investigation combining geophysical, geochemical, and field evidence. J Geophys Res Solid Earth 108:ECV 2-1–ECV 2-14

Devey CW, Scientific Shipboard Party (2013) SoMARTherm: the Mid-Atlantic ridge 13–33 °S. Cruise No. MSM25. Leitstelle Deutsche Forschungsschiffe, Universität Hamburg, 113 p

Devey CW, German C, Haase K, Lackschewitz K, Melchert B, Connelly D (2010) The relationships between volcanism, tectonism, and hydrothermal activity on the southern equatorial Mid-Atlantic Ridge. In: Rona PA, Devey CW, Dyment J, Murton BJ (eds) Diversity of hydrothermal systems on slow spreading ocean ridges, vol 188. American Geophysical Union, Geophys Monograph, pp 133–152

Dick HJB, Natland JH, Alt JC, Bach W, Bideau D, Gee JS, Haggas S, Hertogen JGH, Hirth G, Holm PM, Ildefonse B, Iturrino GJ, John BE, Kelley DS, Kikawa E, Kingdon A, LeRoux PJ, Maeda J, Meyer PS, Miller DJ, Naslund HR, Niu Y-L, Robinson PT, Snow J, Stephen RA, Trimby PW, Worm H-U, Yoshinobu A (2000) A long in situ section of the lower ocean crust: results of ODP Leg 176 drilling at the Southwest Indian Ridge. Earth Planet Sci Lett 179:31–51

Edmonds HN, Michael PJ, Baker ET, Connelly DP, Snow JE, Langmuir CH, Dick HJB, Muhe R, German CR, Graham DW (2003) Discovery of abundant hydrothermal venting on the ultraslow-spreading Gakkel ridge in the Arctic Ocean. Nature 421:252–256

Escartín J, Soule SA, Cannat M, Fornari DJ, Düşünür D, Garcia R (2014) Lucky strike seamount: Implications for the emplacement and rifting of segment-centered volcanoes at slow spreading mid-ocean ridges. Geochem Geophys Geosyst 15:4157–4179

Escartín J, Mével C, Petersen S, Bonnemains D, Cannat M, Andreani M, Augustin N, Bezos A, Chavagnac V, Choi Y et al (2017) Tectonic structure, evolution, and the nature of oceanic core complexes and their detachment fault zones (13°20'N and 13°30'N, Mid-Atlantic Ridge). Geochem Geophys Geosyst 18(4):1451–1482. https://doi.org/10.1002/2016GC006775

Fontaine FJ, Cannat M, Escartín J, Crawford WC (2014) Along-axis hydrothermal flow at the axis of slow spreading Mid-Ocean Ridges: insights from numerical models of the Lucky Strike vent field (MAR). Geochem Geophys Geosyst 15:2918–2931

Fouquet Y (1997) Where are the large hydrothermal sulphide deposits in the oceans? Phil Trans Roy Soc Math Phys Eng Sci 355:427–441

Fournier R (1987) Conceptual models of brine evolution in magmatic-hydrothermal systems. US Geol Surv Prof Pap 1350:1487–1506

France L, Ildefonse B, Koepke J (2009) Interactions between magma and hydrothermal system in Oman ophiolite and in IODP Hole 1256D: fossilization of a dynamic melt lens at fast spreading ridges. Geochem Geophys Geosyst 10:Q10O19. https://doi.org/10.1029/2009gc002652

France L, Koepke J, Ildefonse B, Cichy SB, Deschamps F (2010) Hydrous partial melting in the sheeted dike complex at fast spreading ridges: experimental and natural observations. Contrib Mineral Petrol 160:683–704

Früh-Green GL, Kelley DS, Bernasconi SM, Karson JA, Ludwig KA, Butterfield DA, Boschi C, Proskurowski G (2003) 30,000 years of hydrothermal activity at the Lost City vent field. Science 301:495–498

German CR, Petersen S, Hannington MD (2016) Hydrothermal exploration of mid-ocean ridges: where might the largest sulfide deposits be forming? Chem Geol 420:114–126

Gillis KM, Coogan LA, Chaussidon M (2003) Volatile element (B, Cl, F) behaviour in the roof of an axial magma chamber from the East Pacific Rise. Earth Planet Sci Lett 213:447–462

Girdler RW, Evans TR (1977) Red Sea heat flow. Geophys J Int 51:245–251

Guney M, Al-Marhoun MA, Nawab ZA (1988) Metalliferous sub-marine sediments of the Atlantis-II-Deep, Red Sea. Can Min Metall Bull 81:33–39

Gurvich EG (2006) Metalliferous sediments of the Red Sea. Metalliferous sediments of the World Ocean: fundamental theory of Deep-Sea hydrothermal sedimentation. Springer, Berlin, pp 127–210

Hannington M, Jamieson J, Monecke T, Petersen S (2010) Modern sea-floor massive sulfides and base metal resources: toward an estimate of global sea-floor massive sulfide potential. Soc Econ Geol Spec Pub 15:317–338

Hannington M, Jamieson J, Monecke T, Petersen S, Beaulieu S (2011) The abundance of seafloor massive sulfide deposits. Geology 39:1155–1158

Hart S, Erlank A, Kable E (1974) Sea floor basalt alteration: some chemical and Sr isotopic effects. Contrib Mineral Petrol 44:219–230

Ito E, Harris DM, Anderson AT (1983) Alteration of oceanic crust and geologic cycling of chlorine and water. Geochim Cosmochim Acta 47:1613–1624

Jambon A, Déruelle B, Dreibus G, Pineau F (1995) Chlorine and bromine abundance in MORB: the contrasting behaviour of the Mid-Atlantic Ridge and East Pacific Rise and implications for chlorine geodynamic cycle. Chem Geol 126:101–117

Jenner FE, O'Neill HSC (2012) Analysis of 60 elements in 616 ocean floor basaltic glasses. Geochem Geophys Geosyst 13(2):Q02005

Kelley DS, Delaney JR (1987) Two-phase separation and fracturing in mid-ocean ridge gabbros at temperatures greater than 700 °C. Earth Planet Sci Lett 83:53–66

Kendrick MA, Arculus R, Burnard P, Honda M (2013) Quantifying brine assimilation by submarine magmas: examples from the Galápagos Spreading Centre and Lau Basin. Geochim Cosmochim Acta 123:150–165

Kendrick MA, Hemond C, Kamenetsky VS, Danyushevsky L, Devey CW, Rodemann T, Jackson MG, Perfit MR (2017) Seawater cycled throughout Earth's mantle in partially serpentinized lithosphere. Nat Geosci 10:222–228. https://doi.org/10.1038/NGEO2902

Kent AJR, Norman MD, Hutcheon ID, Stolper EM (1999a) Assimilation of seawater-derived components in an oceanic volcano: evidence from matrix glasses and glass inclusions from Loihi seamount, Hawaii. Chem Geol 156:299–319

Kent AJR, Clague DA, Honda M, Stolper EM, Hutcheon ID, Norman MD (1999b) Widespread assimilation of a seawater-derived component at Loihi Seamount, Hawaii. Geochim Cosmochim Acta 63:2749–2761

Kent AJR, Peate DW, Newman S, Stolper EM, Pearce JA (2002) Chlorine in submarine glasses from the Lau Basin: seawater contamination and constraints on the composition of slab-derived fluids. Earth Planet Sci Lett 202:361–377

Klinkhammer G, Bender M, Weiss RF (1977) Hydrothermal manganese in the Galapagos Rift. Nature 269:319–320

Laurila TE, Hannington MD, Petersen S, Garbe-Schönberg D (2014) Early depositional history of metalliferous sediments in the Atlantis II Deep of the Red Sea: evidence from rare earth element geochemistry. Geochim Cosmochim Acta 126:146–168

le Roux PJ, Shirey SB, Hauri EH, Perfit MR, Bender JF (2006) The effects of variable sources, processes and contaminants on the composition of northern EPR MORB (8–10°N and 12–14°N): evidence from volatiles (H_2O, CO_2, S) and halogens (F, Cl). Earth Planet Sci Lett 251:209–231

Lein AY, Bogdanov YA, Maslennikov V, Li S, Ulyanova N, Maslennikova S, Ulyanov A (2010) Sulfide minerals in the Menez Gwen nonmetallic hydrothermal field (Mid-Atlantic Ridge). Lithol Mineral Resour 45:305–323

Linke P, Schmidt M, Rohleder M, Al-Barakati A, Al-Farawati R (2015) Novel online digital video and high-speed data broadcasting via standard coaxial cable onboard marine operating vessels. Mar Technol Soc Bull 49:7–18

Marcon Y, Sahling H, Borowski C, dos Santos FC, Thal J, Bohrmann G (2013) Megafaunal distribution and assessment of total methane and sulfide consumption by mussel beds at Menez Gwen hydrothermal vent, based on geo-referenced photomosaics. Deep Sea Res Part I 75:93–109

McDonough WF, Sun SS (1995) The composition of the Earth. Chem Geol 120:223–253

Metz D, Augustin N, van der Zwan FM, Bantan RA, Al-Aidaroos AM (2013) Mabahiss Mons, 25.5 °N Red Sea Rift: tectonics and volcanism of a large submarine dome volcano. In: EGU general assembly conference abstracts, vol 15, p 10487

Michael PJ, Cornell WC (1998) Influence of spreading rate and magma supply on crystallization and assimilation beneath mid-ocean ridges: evidence from chlorine and major element chemistry of mid-ocean ridge basalts. J Geophys Res 103:18325–18356

Michael PJ, Schilling J-G (1989) Chlorine in mid-ocean ridge magmas: evidence for assimilation of seawater-influenced components. Geochim Cosmochim Acta 53:3131–3143

Mitchell NC, Ligi M, Ferrante V, Bonatti E, Rutter E (2010) Submarine salt flows in the central Red Sea. Geol Soc Am Bull 122:701–713

Monin A, Plakhin E, Podrazhansky A, Sagalevich A, Sorokhtin O (1981) Visual observations of the Red Sea hot brines. Nature 291:222–225

Monin A, Litvin V, Podrazhansky A, Sagalevich A, Sorokhtin O, Voitov V, Yastrebov V, Zonenshain L (1982) Red sea submersible research expedition. Deep Sea Res Part A Oceanographic Res Papers 29(3):361–373

Perfit MR, Cann JR, Fornari DJ, Engels J, Smith DK, Ian Ridley W, Edwards MH (2003) Interaction of sea water and lava during submarine eruptions at mid-ocean ridges. Nature 426:62–65

Pertsev A, Bortnikov N, Vlasov E, Beltenev V, Dobretsova I, Ageeva O (2012) Recent massive sulfide deposits of the Semenov ore district, Mid-Atlantic Ridge, 13°31′ N: associated rocks of the oceanic core complex and their hydrothermal alteration. Geol Ore Deps 54:334–346

Petersen S, Herzig P, Hannington MD (2000) Third dimension of a presently forming VMS deposit: TAG hydrothermal mound, Mid-Atlantic Ridge, 26 °N. Mineral Deposita 35:233–259

Petersen S, Kuhn K, Kuhn T, Augustin N, Hékinian R, Franz L, Borowski C (2009) The geological setting of the ultramafic-hosted Logatchev hydrothermal field (14°45′ N, Mid-Atlantic Ridge) and its influence on massive sulfide formation. Lithos 112:40–56

Pierret MC, Clauer N, Bosch D, Blanc G, France-Lanord C (2001) Chemical and isotopic (87Sr/86Sr, δ18O, δD) constraints to the formation processes of Red-Sea brines. Geochim Cosmochim Acta 65:1259–1275

Pierret M, Clauer N, Bosch D, Blanc G (2010) Formation of Thetis Deep metal-rich sediments in the absence of brines, Red Sea. J Geochem Explor 104:12–26

Rona PA, Klinkhammer G, Nelsen TA, Trefry JH, Elderfield H (1986) Black smokers, massive sulphides and vent biota at the Mid-Atlantic Ridge. Nature 321:33–37

Saal AE, Hauri EH, Langmuir CH, Perfit MR (2002) Vapour under saturation in primitive mid-ocean-ridge basalt and the volatile content of Earth's upper mantle. Nature 419:451–455

Schmidt M, Linke P, Esser D (2013a) Recent development in IR sensor technology for monitoring subsea methane discharge. Mar Technol Soc Bull 47:27–36

Schmidt M, Al-Farawati R, Al-Aidaroos A, Kürten B (eds) (2013b) RV PELAGIA cruise report 64PE350/64PE351. Berichte aus dem Helmholtz-Zentrum für Ozeanforschung Kiel (GEOMAR) 5

Schmidt M, Al-Farawati R, Botz R (2015) Geochemical classification of brine-filled Red Sea deeps. In: Rasul NMA, Stewart ICF (eds) The Red Sea: the formation, morphology, oceanography and environment of a young ocean basin. Springer Earth System Sciences, Berlin, pp 219–233

Schoell M, Hartmann M (1973) Detailed temperature structure of the hot brines in the Atlantis II Deep area (Red Sea). Mar Geol 14:1–14

Schramm B, Devey CW, Gillis KM, Lackschewitz K (2005) Quantitative assessment of chemical and mineralogical changes due to progressive low-temperature alteration of East Pacific Rise basalts from 0 to 9 Ma. Chem Geol 218:281–313

Soule SA, Fornari DJ, Perfit MR, Ridley WI, Reed MH, Cann JR (2006) Incorporation of seawater into mid-ocean ridge lava flows during emplacement. Earth Planet Sci Lett 252:289–307

Staudigel H, Plank T, White B, Schmincke HU (1996) Geochemical fluxes during seafloor alteration of the basaltic upper oceanic Crust: DSDP sites 417 and 418. In: Bebout GE, Scholl DW, Kirby SH, Platt JP (eds) Subduction top to bottom. American Geophysical Union, Washington, DC, pp 19–38

Sun WD, Binns RA, Fan AC, Kamenetsky VS, Wysoczanski R, Wei GJ, Hu YH, Arculus RJ (2007) Chlorine in submarine volcanic glasses from the eastern Manus Basin. Geochim Cosmochim Acta 71:1542–1552

Swallow JC, Crease J (1965) Hot salty water at the bottom of the Red Sea. Nature 205:165–166

Szitkar F, Petersen S, Caratori Tontini F, Cocchi L (2015) High-resolution magnetics reveal the deep structure of a volcanic-arc-related basalt-hosted hydrothermal site (Palinuro, Tyrrhenian Sea). Geochem Geophys Geosyst 16:1950–1961

van der Zwan FM (2014) Hydrothermal activity at slow-spreading mid-ocean ridges: evidence from chlorine in basalt. PhD thesis, Christian-Albrechts-Universität Kiel

van der Zwan FM, Fietzke J, Devey CW (2012) Precise measurement of low (<100 ppm) chlorine concentrations in submarine basaltic glass by electron microprobe. J Analyt At Spectrom 27:1966–1974

van der Zwan FM, Devey CW, Augustin N, Almeev RR, Bantan RA, Basaham A (2015) Hydrothermal activity at the ultraslow- to slow-spreading Red Sea Rift traced by chlorine in basalt. Chem Geol 405:63–81

van der Zwan FM, Devey CW, Hansteen TH, Almeev RR, Augustin N, Frische M, Haase KM, Basaham A, Snow JE (2017) Lower crustal hydrothermal circulation at slow-spreading ridges: Evidence from chlorine in Arctic and South Atlantic basalt glasses and melt inclusions. Contrib Mineral Petrol 172(11–12):97. https://doi.org/10.1007/s00410-017-1418-1

Von Damm K, Lilley M, Shanks W III, Brockington M, Bray A, O'Grady K, Olson E, Graham A, Proskurowski G (2003) Extraordinary phase separation and segregation in vent fluids from the southern East Pacific Rise. Earth Planet Sci Lett 206:365–378

Wanless V, Perfit M, Ridley W, Klein E (2010) Dacite petrogenesis on mid-ocean ridges: evidence for oceanic crustal melting and assimilation. J Petrol 51:2377–2410

Whitmarsh RB, Weser OE, Ross DA (1974) Initial reports of the deep sea drilling project, vol 23. U.S. Government Printing Office, Washington, DC, pp 35–56

Yoshikawa S, Okino K, Asada M (2012) Geomorphological variations at hydrothermal sites in the southern Mariana Trough: relationship between hydrothermal activity and topographic characteristics. Mar Geol 303:172–182